Available online at www.sciencedirect.com
SCIENCE DIRECT®
PERGAMON
Applied Radiation and Isotopes 59 (2003) 17–25
Applied Radiation and Isotopes
www.elsevier.com/locate/apradiso

Gamma-ray-computed tomography to investigate compaction on sewage-sludge-treated soil

Luiz F. Pires[a,*], Jose R. de Macedo[b], Manoel D. de Souza[c], Osny O.S. Bacchi[a], Klaus Reichardt[a]

[a] *Center for Nuclear Energy in Agriculture, USP, C.P. 96, C.E.P., SP 13.400-970 Piracicaba, Brazil*
[b] *Embrapa Soils, Rua Jardim Botânico, 1024, C.E.P., RJ 22.260-000 Rio de Janeiro, Brazil*
[c] *Embrapa Environment, C.P. 69, C.E.P., SP 13.820-000 Jaguariúna, Brazil*

Received 21 March 2003; accepted 23 April 2003

Abstract

Soil compaction is one of the fundamental parameters to evaluate the environmental impact of agricultural machinery traffic on soils. Compaction causes modifications on soil physical properties such as changes in porosity and structure that are related to soil water movement and gas exchange The objective of this work was to evaluate soil surface sealing after sewage-sludge application, and the influence of agricultural machinery traffic, through computed tomography. A first generation tomograph was used having a ^{137}Cs source and a 3 in × 3 in NaI(Tl) scintillation crystal detector coupled to a photomultiplier tube. Image analysis and tomographic unit profiles could successfully be used for the detection of soil surface sealing and soil compaction due to machinery traffic associated to sewage-sludge application.

Keywords: Gamma-ray-computed tomography; Soil compaction; Soil surface sealing

1. Introduction

Gamma-ray-computed tomography (CT) is a non-destructive technique suitable to investigate different phenomena. The first studies were performed in medical science, and lately with the success of the technique, the CT began to be used in other areas. Coles et al. (1998) developed the computed microtomography employing synchrotron X-ray sources to obtain pore level imaging of fluid transport. Stenstrom et al. (1998) applied CT to investigate morphological changes in small animals. Braz et al. (2000) analyzed dental anatomy and some restorative materials through X-ray microtomography. Schroer (2001) combined fluorescence microanalysis with tomographic techniques to obtain map element distributions within a sample. In soil science, the first studies were introduced to measure soil density, soil water content, and soil water movement (Crestana et al., 1985; Hainsworth and Aylmore, 1983; Petrovic et al., 1982). Recently, Macedo et al. (1999) utilized X-ray microtomography, also to characterize soil physical properties, and Brandsma et al. (1999) applied the technique to determine soil macroporosity by chemical mapping. Fante Júnior et al. (2002) evaluated the occurrence of soil compaction caused by different soil management practices.

Soil compaction is one of the fundamental aspects to evaluate the environmental impact of agricultural machinery traffic on soils. It can also occur due to natural forces acting on the soil or several anthropogenic activities (Pagliai et al., 1998; Marsili et al., 1998). Soil compaction causes modifications on soil physical properties such as changes in porosity and structure that are related to soil water and gas movement. Soil porosity modification has consequences as the decrease of the water infiltration rate and possibility of the occurrence

*Corresponding author. Tel.: +55-1934294600; fax: +55-1934294610.
E-mail address: lfpires@cena.usp.br (L.F. Pires).

0969-8043/03/$ - see front matter © 2003 Elsevier Ltd. All rights reserved.
doi:10.1016/S0969-8043(03)00145-3

of furrow erosion. Soil structure is one of the most important properties affecting crop production because it determines the depth that roots can explore, the amount of water that can be stored and the movement of air, water, nutrients, and soil fauna.

According to Baver et al. (1973) soil-surface sealing is a specific physical modification of the soil, and this phenomenon is a result of the impact of raindrops on bare soil, mainly after soil preparation operations, or during the initial growth stages of the crop. The impact energy of raindrops promotes the disintegration of soil aggregates by mass expansion and explosion of trapped air, promoting the dispersion and orientation of the finest particles, which infiltrate along with water, plugging smaller pores. During the drying process, deposition, migration, and orientation lead to the formation of a fine hard surface layer. This layer reduces the time for surface flooding, increasing run-off volume, favoring laminar and furrow erosions (Pagliai and Vignozzi, 1998; Pla, 1985).

During the last decade, many studies have been carried out on the application of sewage sludge as fertilizer and a soil conditioner (Tsutiya, 2001). Several results have shown that the application of sewage sludge promotes a significant change on the soil surface, causing an additional surface sealing (Pires et al., 2002; Macedo, 2002), and modifications in soil physical properties (Macedo et al., 2001; Marciano, 1999; Logan et al., 1996; Bernardes, 1982).

The objective of this work was to evaluate soil-surface sealing through CT after sewage-sludge application, and the influence of agricultural machinery traffic on sewage-sludge-treated soil.

2. Theory

When a gamma-ray beam passes through an homogeneous material of thickness x (cm) several electromagnetic interaction processes occur (Wang et al., 1975), and the transmitted photons follow the Beer–Lambert law

$$N = N_0 \exp \oint_S \left[-\left(\frac{\mu}{\rho}\right)\rho x \right] \mathrm{d}s, \tag{1}$$

where N and N_0 (number of photons $\mathrm{m^{-2}\,s^{-1}}$) are, respectively, the emerging and incident monoenergetic photon flux densities of energy E_γ (keV), μ ($\mathrm{cm^{-1}}$) and μ/ρ ($\mathrm{cm^2\,g^{-1}}$) are the linear and mass attenuation coefficients, and ρ ($\mathrm{g\,cm^{-3}}$) is the physical density of the material.

The mass attenuation coefficient can be obtained from Eq. (1), since N, N_0, ρ and x can be measured:

$$\left(\frac{\mu}{\rho}\right) = \left[\frac{1}{\rho x}\ln\left(\frac{N_0}{N}\right)\right]. \tag{2}$$

It measures the photon absorption or scatter probability per unit length while interacting within the sample, and is proportional to the cross-section per electron κ_e ($\mathrm{cm^2}$/electron), therefore,

$$\left(\frac{\mu}{\rho}\right) = \frac{\kappa_e Z N_{adv}}{A}, \tag{3}$$

where Z is the atomic number, N_{adv} Avogadro's number, and A the atomic mass of the material.

Values of the attenuation coefficient of the soil in the CT image can be associated with numbers called tomographic units (TU) that are numerical values assigned to gray levels (Naime et al., 2000; Crestana and Vaz, 1998). TU takes the air as the media with the minimum possible μ value. It is related to the Hounsfield unit (HU) that takes the water as a reference media for which HU = 0. The relation between the TU and the μ of the sample is given by

$$\mathrm{TU}(E_\gamma) = \alpha\mu(E_\gamma) = \alpha\left[\left(\frac{\mu_s(E_\gamma)}{\rho_s}\right)\rho_s + \left(\frac{\mu_w(E_\gamma)}{\rho_w}\right)\theta\right], \tag{4}$$

where α represents the correlation between the linear attenuation coefficient and TU, μ_s/ρ_s and μ_w/ρ_w ($\mathrm{cm^2\,g^{-1}}$) are the mass attenuation coefficients of soil and water, respectively, and θ ($\mathrm{cm^3\,cm^{-3}}$) is the volumetric soil water content.

The variations in TU values correspond to differences in soil density and water content. When the soil sample is dry or its water content is uniformly distributed, the TU distribution reflects only the soil bulk density distribution, and consequently, the soil image obtained through the CT can be used to determine soil compaction (Macedo et al., 2000):

$$\rho_s = \frac{\mathrm{TU}}{\alpha\left[(\mu_s/\rho_s) + (\mu_w/\rho_w)\Phi\right]}, \tag{5}$$

where Φ ($\mathrm{g\,g^{-1}}$) represents the gravimetric soil water content.

3. Material and methods

3.1. Soil samples and preparation

The sewage-sludge field experiment was established in 1998 at the National Center for Environment Research (CNPMA-Embrapa) [22°41′S, 47°00′W, 570 m above mean sea], Jaguariúna, SP, Brazil, on a medium-clayey soil, a dark-red Latosol according to the Brazilian Soil Science Society classification. The experiment consists of four treatments [three sludge rates + one control (absolute control)], using split–plot blocks with three replicates. The term absolute control refers to the control plots that did not receive neither sewage sludge nor inorganic fertilizer. The rates of sludge application were calculated on the basis of dry weight of mineral

nitrogen, corresponding to: 10, 40 and 80 kg m^{-2} of N and here identified as 1N, 4N and 8N, respectively.

The vehicle utilized for soil preparation practices and sewage-sludge application was a tractor (MF 275—2 × 4) of 2.553 kg. The vehicle passed none and twice on the same track while performing soil preparation and sewage-sludge application.

For CT analysis, 12 soil samples were collected at the soil surface using cylinders of 5 cm high and 5 cm diameter, nine of which from areas receiving different rates of sewage sludge, in order to obtain tomographic images. Average dry bulk density was measured by the volumetric ring method (Embrapa, 1998) and CT methods by taking samples of soil below tractor tracks after none and two passages.

3.2. Tomographic system

A first-generation gamma-ray CT system was used in this experiment, having a fixed source–detector arrangement in which soil samples are translated and rotated. Translation and rotation movements were controlled by a microcomputer through coupling interfaces. The radioactive source is ^{137}Cs with an activity of 7.4 GBq that emits monoenergetic photons (661.6 keV). The detector is a 3 in × 3 in NaI(Tl) scintillation crystal coupled to a photomultiplier tube. Circular lead collimators with a diameter of 1 mm were utilized for both source and detector. The acquired data for soil samples were stored in a PC memory and a reconstruction image algorithm was used to process images and display them on the computer screen (Fig. 1).

The calibration of the tomographic system was obtained through the correlation between linear attenuation coefficients of different homogeneous materials (water, alcohol, nylon, acrylic, aluminum and brass) using the gamma-ray transmission method and the respective tomographic units (Pires et al., 2002; Macedo et al., 1998; Cássaro, 1994).

The tomographic images of soil samples were taken at vertical planes crossing the center of the sample, and TU values were converted into soil bulk density profiles using Eq. (5).

4. Results and discussion

The values obtained for linear and mass attenuation coefficients of the soil ($\mu_s = 0.0836 \pm 0.0025$ cm^2 g^{-1}) and water ($\mu_w = 0.0850 \pm 0.0005$ cm^2 g^{-1}) are in accordance with those found in the literature for 661.6 keV photons of ^{137}Cs (Ferraz and Mansell, 1979).

The average soil bulk density values obtained by both volumetric ring and CT methods are shown in Table 1.

Table 1
Average values of soil bulk density (ρ_s), density of the layer presenting soil surface sealing (ρ_{crust}) and density of the compacted soil layer (ρ_{cc}) for samples of treatments (T_{abs}: absolute control; 1N, 4N and 8N: rates of sewage sludge)

Treatment	ρ_s (g cm^{-3})[a]	ρ_{crust} (g cm^{-3})[b]	ρ_{cc} (g cm^{-3})[b]
T_{abs}	1.08 ± 0.07	1.12 ± 0.08	1.11 ± 0.08
1N	1.05 ± 0.08	1.15 ± 0.02	1.15 ± 0.06
4N	1.02 ± 0.12	1.20 ± 0.04	1.19 ± 0.11
8N	1.09 ± 0.11	1.22 ± 0.03	1.24 ± 0.12

[a] Measured by the volumetric ring method.
[b] Measured by the CT method.

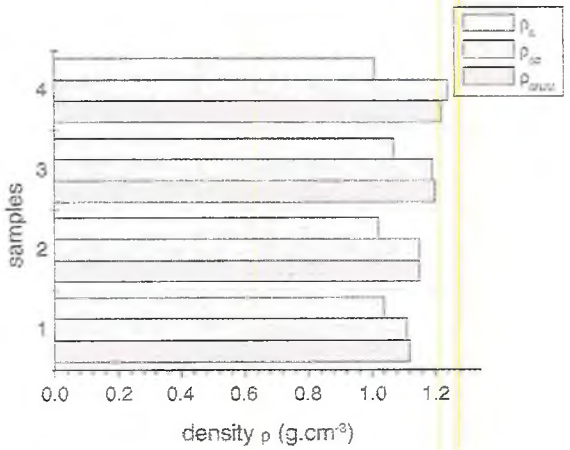

Fig. 2. Average soil bulk density for not compacted soil (ρ_s), for samples presenting surface sealing (ρ_{crust}) and for compacted soil samples (ρ_{cc}).

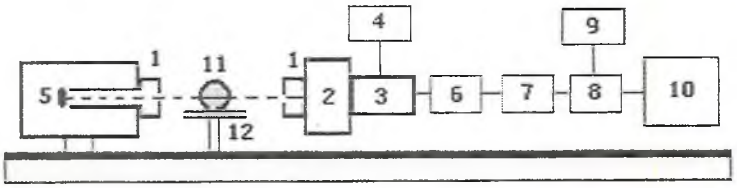

Fig. 1. Schematic diagram of the first-generation tomograph used for CT measurements: (1) lead collimators; (2) NaI(Tl) detector; (3) photomultiplier; (4) high-voltage unit; (5) ^{137}Cs source; (6) amplifier; (7) monocanal analyzer; (8) counter; (9) timer; (10) microcomputer; (11) soil sample, and (12) rotation–translation system.

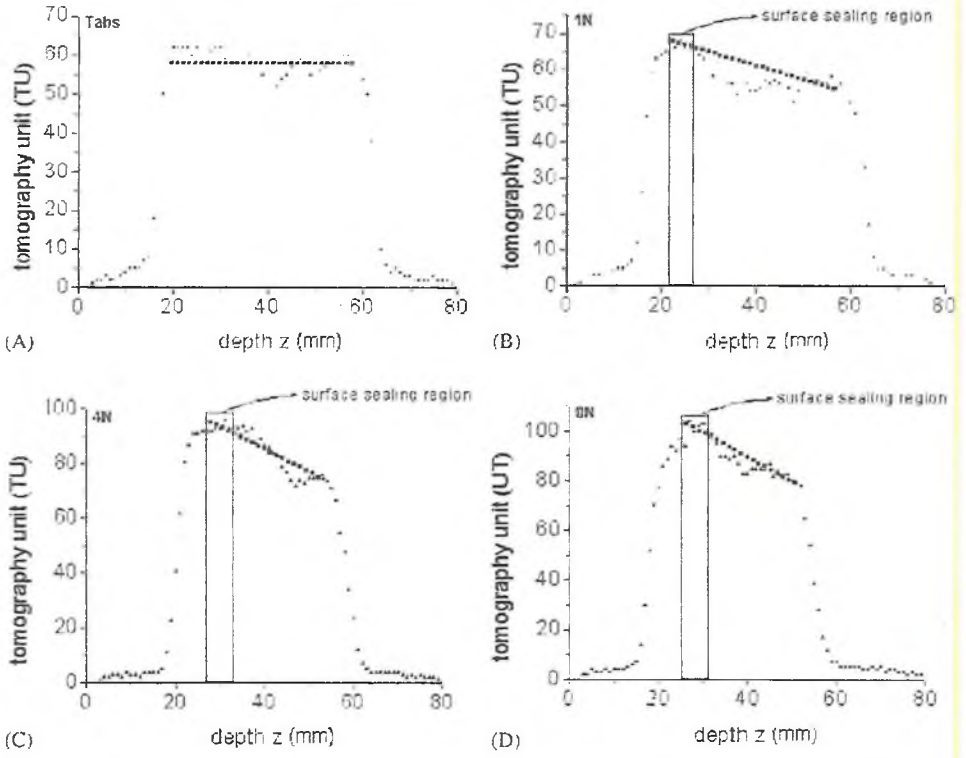

Fig. 3. Vertical profile of tomographic units obtained for samples that did not receive wheel tractor passages during sewage-sludge application: (A) absolute control (without any treatment); (B) 1N sample; (C) 4N sample; and (D) 8N sample. In these samples the presence of soil surface sealing can be observed.

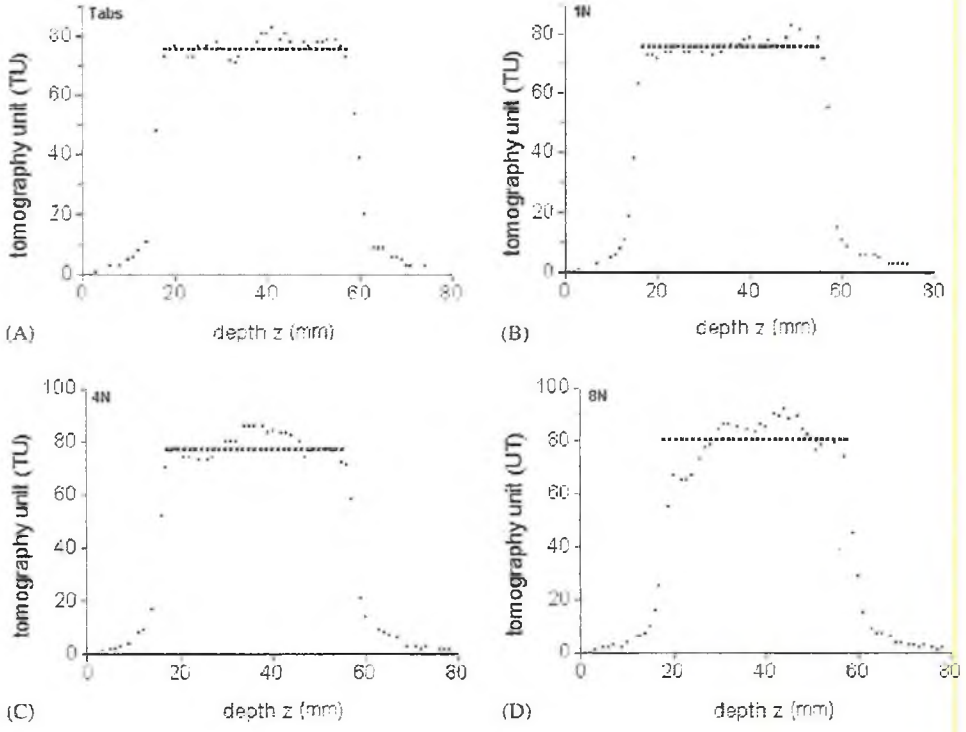

Fig. 4. Vertical profile of tomographic unit obtained for samples that received two-wheel tractor passages during sewage-sludge application: (A) absolute control; (B) 1N sample; (C) 4N sample and (D) 8N sample. For these samples soil-surface sealing is disguised by bulk soil compaction caused by the tractor passage.

Values of volumetric ring density ρ_s are averages of nine rings per treatment. The average data of the density of the sealed crust ρ_{crust} obtained by CT correspond to the average of three samples and to a surface thin layer of about 2–4 mm. Column 4 shows the average density values of ρ_{cc}, which correspond to compacted soil samples that were exposed to two-wheel tractor passages.

Fig. 2 indicates that average bulk density values of the soil surface sealing region (ρ_{crust}) and compacted soil region (ρ_{cc}) do not differ. These results show that for the sample that presents compaction it was not possible to identify the presence of soil surface sealing, probably as a consequence of increment of the soil bulk density due to wheel compaction, which disguised the sealing. The higher densities ρ_{crust} and ρ_{cc} in relation to ρ_s (not compacted soil) indicate the presence of soil surface sealing as a result of sewage-sludge application (see Pires et al., 2002) and soil compaction caused by agricultural machinery.

Analyzing Table 1 it can be seen that with the increase of the sewage-sludge rate, ρ_{crust} increases, reaching values that are larger than those obtained for deeper layers (Figs. 3B–D). For the compacted samples (ρ_{cc}) that received the same treatments (1N, 4N and 8N) of the soil samples with surface sealing, the values of TU obtained in depth practically did not differ from those of the soil surface (Figs. 4B–D). This is an indication that the approximate homogeneity of TU values is a

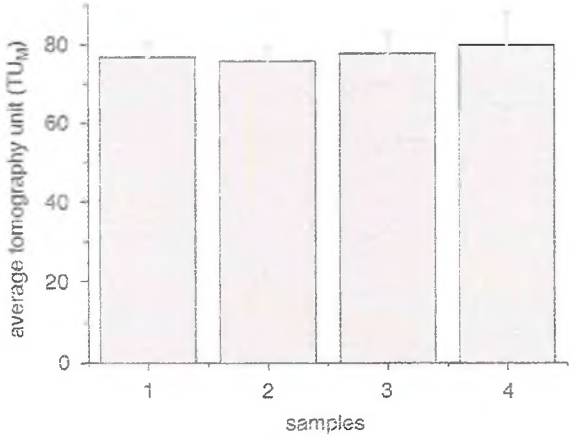

Fig. 5. Histogram of tomographic unit values obtained for the samples (1 (absolute control), 2 (1N sample), 3 (4N sample), 4 (8N sample)) that received two-wheel tractor passages during sewage-sludge application. Vertical bars indicate one standard deviation.

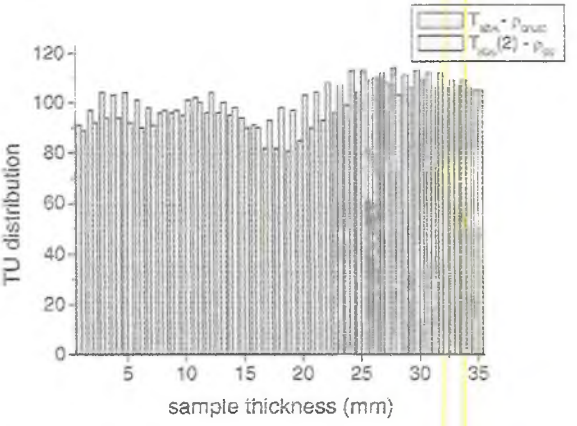

Fig. 7. Tomographic units distributions for the absolute control samples: T_{abs} (not submitted to tractor passages) and $T_{abs}(2)$ (two-wheel tractor passages).

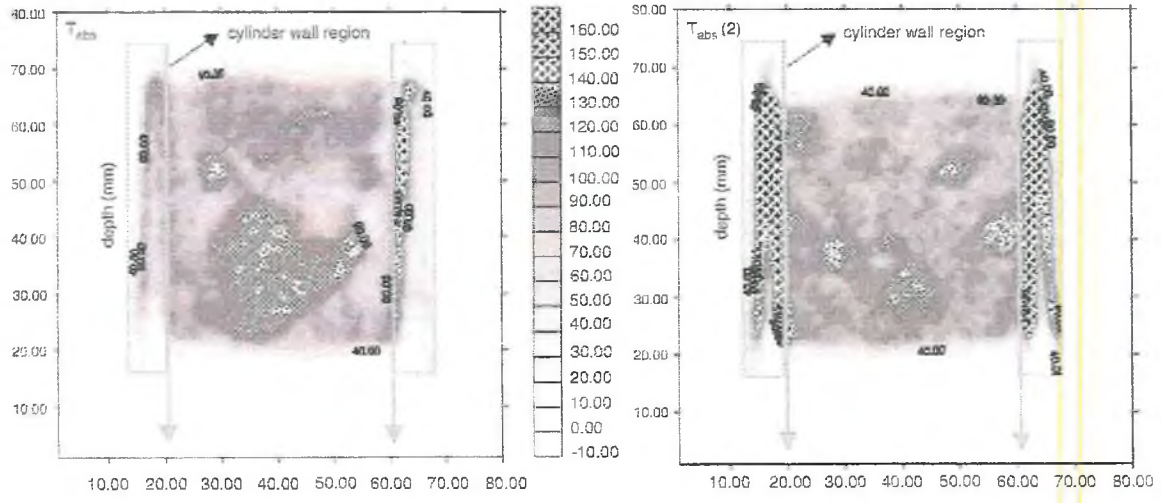

Fig. 6. Tomographic images for the absolute control samples. T_{abs} and $T_{abs}(2)$ represent samples not submitted to tractor passages and submitted to two-wheel tractor passages, respectively.

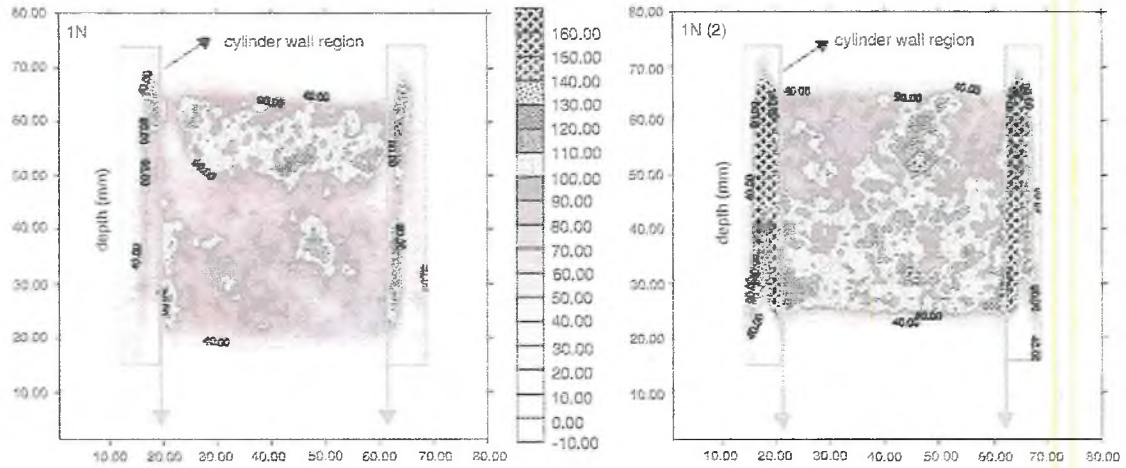

Fig. 8. Tomographic images from the 1N samples. 1N and 1N(2) represent samples not submitted and submitted to two-wheel tractor passages, respectively.

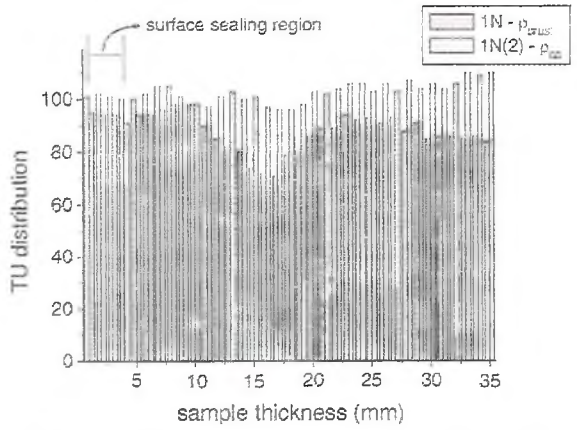

Fig. 9. Tomographic units distributions for the 1N samples: 1N (not submitted to tractor passages) and 1N(2) (two-wheel tractor passages).

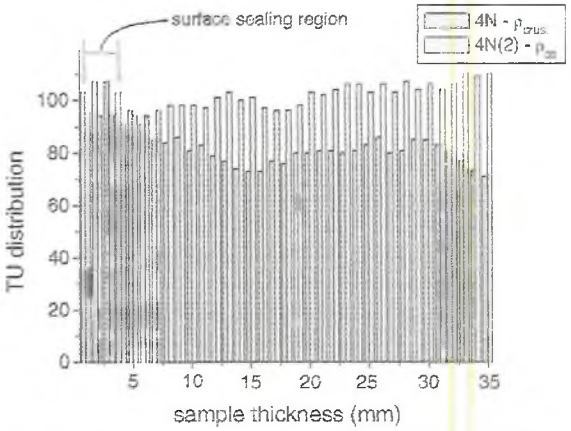

Fig. 11. Tomographic units distributions for the 4N samples: 4N (not submitted to tractor passages) and 4N(2) (two-wheel tractor passages).

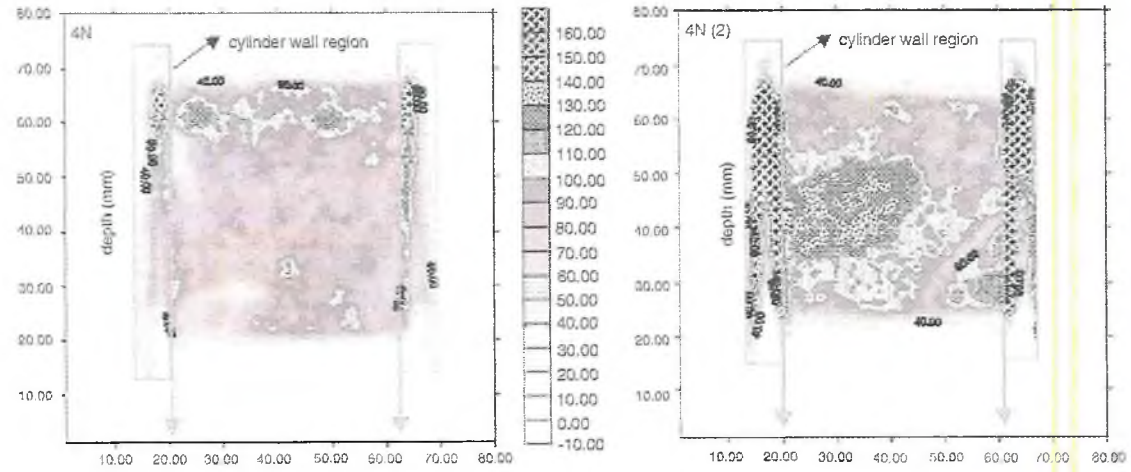

Fig. 10. Tomographic images from the 4N samples. 4N and 4N(2) represent samples not submitted and submitted to two-wheel tractor passages, respectively.

consequence of the effect of the tractor passage during soil preparation and sewage-sludge application, disguising the surface sealing.

In order to confirm the results obtained in Fig. 4 an average TU histogram (Fig. 5) was constructed that shows the values for the different treatments (T_{abs}, 1N, 4N, and 8N). These values practically did not present differences between treatments, indicating the formation of homogeneously compacted layers.

Figs. 6–13 represent a comparison between soil samples submitted to none and two-wheel passages. Observing the CT images it can be seen that for the samples that were not submitted to tractor passages there are less compacted regions in relation to the samples that were submitted to two passages.

Fig. 6 shows the images obtained for the absolute control samples. It can be seen that there is no formation of a surface compacted layer, confirming that for T_{abs} samples the CT analysis is capable of identifying the absence of soil surface sealing. Fig. 7 displays vertical scans of these images to facilitate the interpretation of the images of Fig. 6.

Fig. 8 shows the tomographic images for the 1N treatment. For samples that did not receive wheel passages a compacted region in the surface can be observed ratifying a possible surface sealing due to sewage-sludge application. On tomographic images of samples submitted to tractor passages it was not possible to observe a compacted region in the surface, because the sample presents compaction due to tractor traffic, which disguises the presence of surface sealing. Vertical scans of these images (Fig. 9) confirm the existence of soil surface sealing for sample 1N, and display an approximately uniform variation of tomographic units for sample 1N(2) ratifying the existence of soil compaction.

Figs. 10–13 show the tomographic images and vertical scans of tomographic units for samples that received sewage sludge at rates 4N and 8N. Through the analyses of images and vertical scans it is possible to detect the same tendency obtained for samples that received sewage sludge as fertilizer at rate 1N. These results confirm the presence of soil surface sealing for samples that did not receive wheel tractor passages and the existence of soil compaction for samples submitted to tractor passages, again disguising soil surface sealing. The variations of density in the soil surface region

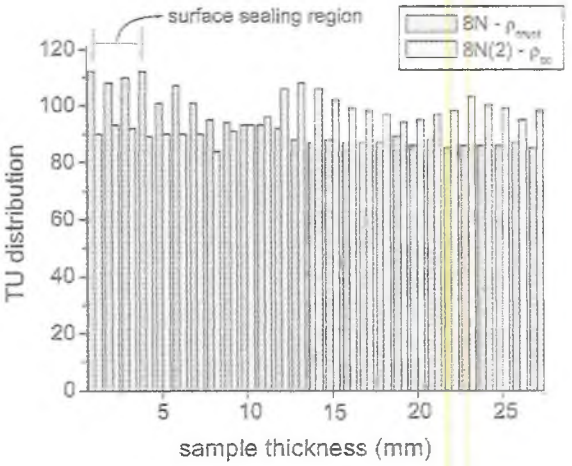

Fig. 13. Tomographic units distributions for the 8N samples: 8N (not submitted to tractor passages) and 8N(2) (two-wheel tractor passages).

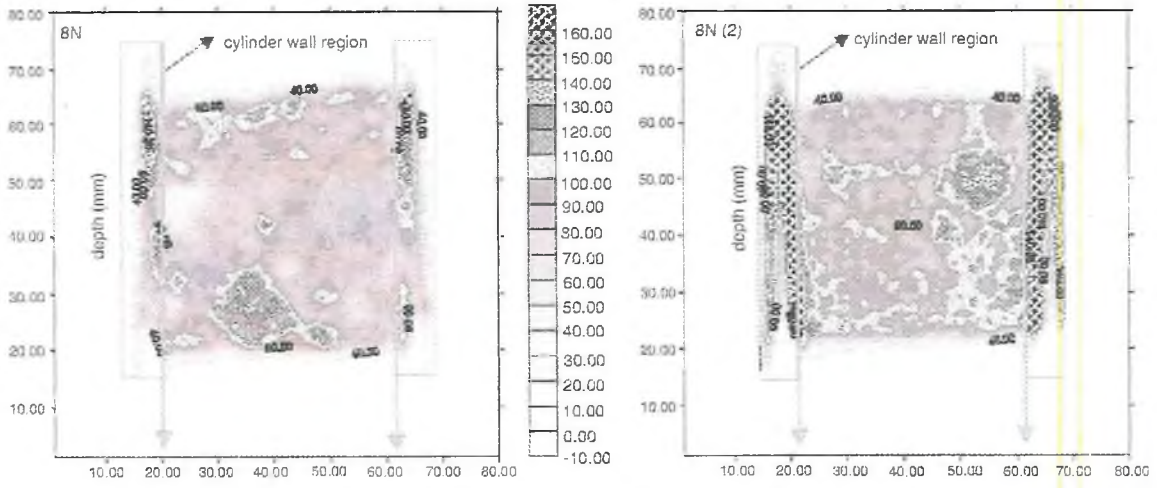

Fig. 12. Tomographic images from the 8N samples. 8N and 8N(2) represent samples not submitted and submitted to two-wheel tractor passages, respectively.

observed for samples that were not submitted to tractor passages (Figs. 8A, 10A and 12A) are, most probably, consequence of soil preparation and sewage-sludge application.

The results obtained in this work confirm the effect of soil compaction due to wheel tractor passages, and that this compaction disguises the presence of surface sealing caused by the sewage-sludge application.

Acknowledgements

We acknowledge FAPESP (Grant Nos. 00/09048-6 and 00/05732-0) for the financial support.

References

Baver, L.D., Gardner, W.J., Gardner, W.R., 1973. Física de suelos. Union Tipográfica Editorial Hispano Americana, Mexico, 529pp.

Bernardes, L.F., 1982. Efeitos da aplicação do lodo de esgoto nas propriedades físicas do solo. Dissertação de mestrado, UNESP/FCAV, Jaboticabal, Brasil, 50pp.

Brandsma, R.T., Fullen, M.A., Hocking, T.J., Allen, J.R., 1999. An X-ray scanning technique to determine soil macroporosity by chemical mapping. Soil Tillage Res. 50, 95–98.

Braz, D., De Oliveira, L.F., Morhy, O.N., Lopes, R.T., 2000. Dental restorative materials analysis using 3D Ray microfocus tomography system. In: VII SARX—Seminario Latino-americano de Análises por Técnicas de Raios-X, Resumos expandidos, São Pedro, Brasil, CD-ROM.

Cássaro, F.A.M., 1994. Tomografia de dupla energia simultânea para caracterização física de um meio poroso deformável. Dissertação de mestrado, EESC/USP, São Carlos, Brasil, 119pp.

Coles, M.E., Hazlett, R.D., Spanne, P., Soll, W.E., Muegge, E.L., Jones, K.W., 1998. Pore level imaging of fluid transport using synchrotron X-ray microtomography. J. Petroleum Sci. Engineer. 19, 55–63.

Crestana, S., Vaz, C.M.P., 1998. Non-invasive instrumentation opportunities for characterizing soil porous systems. Soil Tillage Res. 47, 19–26.

Crestana, S., Mascarenhas, S., Pozzi-mucelli, R.S., 1985. Static and dynamic three-dimensional studies of water in soil using computerized tomography scanning. Soil Sci. 140, 326–331.

Embrapa, 1998. Manual de análise de solos. Centro Nacional de Pesquisa de Solos, Rio de Janeiro, Brasil, 156pp.

Fante Júnior, L., Oliveira, J.C.M., Bassoi, L.H., Vaz, C.M.P., Macedo, A., Bacchi, O.O.S., Reichardt, K., 2002. Tomografia computadorizada na avaliação da densidade de um solo do semi-árido Brasileiro. Braz. J. Soil Sci. 26, 835–842.

Ferraz, E.S.B., Mansell, R.S., 1979. Determining water content and bulk density of soil by gamma ray attenuation methods. Technical Bulletin, No. 807. IFAS, Flórida, 51p.

Hainsworth, J.M., Aylmore, L.A.G., 1983. The use of computer-assisted tomography to determine spatial distribution of soil water content. Aust. J. Soil. Res. 21, 435–440.

Logan, T.J., Harrison, B.J., McAvoy, D.C., Greff, J.A., 1996. Effects of olestra in sewage sludge on soil physical properties. J. Environ. Qual. 25, 153–161.

Macedo, J.R., 2002. Selamento superficial e atributos físicos e hídricos em solo tratado com lodo de esgoto. Tese de doutorado, CENA/USP, Piracicaba, Brasil, 87pp.

Macedo, A., Crestana, S., Vaz, C.M.P., 1998. X-ray microtomography to investigate thin layers of soil clod. Soil Tillage Res. 49, 249–253.

Macedo, A., Vaz, C.M.P., Naime, J.M., Cruvinel, P.E., Crestana, S., 1999. X-ray microtomography to characterize the physical properties of soil and particulate systems. Powder Technol. 101, 178–182.

Macedo, A., Vaz, C.M.P., Naime, J.M., Cruvinel, P.E., Bassoi, L.H., Bacchi, O.O.S., Fante Júnior, L., Oliveira, J.C.M., 2000. The use of tomography to evaluate soil compaction in a red yellow podzolic area of the Brazilian northeast. In: Cruvinel, P.E., Colnago, L.A. (Eds.), Agricultural Tomography. Embrapa-CNPDIA, São Carlos, Brasil, pp. 105–109.

Macedo, J.R., Pires, L.F., Reichardt, K., De Souza, M.D., Bacchi, O.O.S., Meneguelli, N.A., 2001. Utilização de biossólido (lodo de esgoto) e sua influência nas propriedades físicas do solo. In: Delgado, R.V. (Ed.), Congreso Latinoamericano de la Ciencia del Suelo, Vol. 15, Resumenes expandidos. SLCS, Havana, Cuba, CD-ROM.

Marciano, C.R., 1999. Incorporação de resíduos urbanos e as propriedades físico-hídricas de um Latossolo Vermelho Amarelo. Tese de doutorado, ESALQ/USP, Piracicaba, Brasil, 93pp.

Marsili, A., Servadio, P., Pagliai, M., Vignozzi, N., 1998. Changes of some physical properties of a clay soil following passage of ruber- and metal-tracked tractors. Soil Tillage Res. 49, 185–199.

Naime, J.M., Cruvinel, P.E., Silva, A.M., Crestana, S., Vaz, C.M.P., 2000. Applications of X and γ-rays dedicated computerized tomography scanner in agriculture. In: Cruvinel, P.E., Colnago, L.A. (Eds.), Agricultural Tomography. Embrapa-CNPDIASão Carlos, São Carlos, Brasil, pp. 96–104.

Pagliai, M., Vignozzi, N., 1998. Use of manure for soil improvement. In: Wallace, A., Terry, R.E. (Eds.), Handbook of Soil Conditiones. Substances that Enhance the Physical Properties of Soil. Marcel Dekker Inc., New York.

Pagliai, M., Rousseva, S., Vignozzi, N., Piovanelli, C., Pellegrini, S., Miclaus, N., 1998. Tillage impact on soil quality. I: soil porosity and related physical properties. Ital. J. Agron. 2, 11–20.

Petrovic, A.M., Siebert, J.E., Rieke, P.E., 1982. Soil bulk density analysis in three dimensions by computed tomographic scanning. Soil Sci. Soc. Am. J. 46, 445–450.

Pires, L.F., Macedo, J.R., Souza, M.D., Bacchi, O.O.S., Reichardt, K., 2002. Gamma-ray computed tomography to characterize soil surface sealing. Appl. Radiat. Isot. 57, 375–380.

Pla, I., 1985. A routine laboratory index to predict the effects of soil sealin on soil and water conservation. In: International Symposium on the Assessment of Soil Surface Sealing and Crusting. ISSS.AISS.IBG, Ghent, Belgium, pp. 154–162.

Schroer, C.G., 2001. Reconstructing X-ray fluorescence microtomograms. Appl. Phys. Lett. 79, 1912–1914.

Stenstrom, M., Olander, B., Carlsson, C.A., Alm Carlsson, G., Lehto-Axtelius, D., Hakanson, R., 1998. The use of computed microtomography to monitor morphological changes in small animals. Appl. Radiat. Isot. 49, 565–570.

Tsutiya, M.T., 2001. Caracteristicas de biossólidos gerados em estações de tratamento de esgoto. In: Bettiol, W., Camargo, O.A. (Eds.), Biossólidos na Agricutura. Jaboticabal, Brasil, pp. 89–131.

Wang, C.H., Willis, D.L., Loveland, W.D., 1975. Characteristics of ionizing radiation. In: Wang, C.H., Willis, D.L., Loveland, W.D. (Eds.), Radiotracer Methodology in the Biological Environmental, and Physical Sciences. Prentice-Hall, Englewood Cliffs, NJ, pp. 39–74.